



High-throughput determination of the composition-dependent interdiffusivities in Cu-rich fcc Cu–Ag–Sn alloys at 1073 K



Huixia Xu^a, Weimin Chen^a, Lijun Zhang^{a,*}, Yong Du^a, Chengying Tang^b

^a State Key Laboratory of Powder Metallurgy, Central South University, Changsha, Hunan 410083, PR China

^b Guangxi Key Laboratory of Information Materials, Guilin University of Electronic Technology, Guilin 541004, PR China

ARTICLE INFO

Article history:

Received 27 February 2015

Received in revised form 3 May 2015

Accepted 6 May 2015

Available online 12 May 2015

Keywords:

Fcc Ag–Cu–Sn alloys

Diffusion

Interdiffusivity

Diffusion couple

Numerical inverse method

Matano–Kirkaldy method

ABSTRACT

Based on the recently developed pragmatic numerical inverse method for determining the composition-dependent interdiffusivities in a ternary system by using a single diffusion couple, high-throughput determination of the interdiffusivities in Cu-rich fcc Cu–Ag–Sn alloys at 1073 K was performed in the present work. The composition-dependent interdiffusivity matrices along the entire diffusion paths of five fcc Cu–Ag–Sn diffusion couples were obtained. The reliability of the interdiffusivities determined by the pragmatic numerical inverse method was first validated by Fick's second law applied to numerical simulation of composition profiles and interdiffusion fluxes for each diffusion couple. The excellent agreement between the simulated results and the experimental data was obtained. In order to further validate their reliability, the traditional Matano–Kirkaldy method was employed to evaluate the interdiffusivities at the intersection point of the diffusion paths for every two diffusion couples. The good agreement between the interdiffusivities determined by the pragmatic numerical inverse method and those by the traditional Matano–Kirkaldy method was also observed. These facts indicate that the interdiffusivities determined by the pragmatic numerical inverse method are reliable.

© 2015 Elsevier B.V. All rights reserved.

1. Introduction

Due to its low melting point, high wetting property and excellent comprehensive performance, the Ag–Cu–Sn solder is recognized to be the most widely used lead-free solder alloy [1–6]. In order to fully understand the microstructure evolution during the welding and the later service processes, for instance, the interfacial reaction and interdiffusion behavior between the solder and substrate, the accurate diffusivity information in the Ag–Cu–Sn system is the prerequisite. Moreover, a project aiming at development of atomic mobility database in the Sn–Ag–Bi–Cu–In–Pb solder alloy via an integration of experimental measurement, DICTRA (Diffusion-Controlled TRAnsformation) simulation and atomistic simulation is currently carried out in our research group. Up to now, the atomic mobility database for liquid phase in Sn–Ag–Bi–Cu–In–Pb solder has been established by Chen et al. [7–9] using a modified Sutherland equation [10] and the phenomenological treatment of diffusion in liquid [11,12]. The established liquid atomic mobility database was also successfully applied to simulate the dissolution of Ag and Cu substrates into liquid solder alloys during the reflow process [9]. However, this is not the case for solid

phases, i.e., face centered cubic (fcc) and intermetallic phases. The major obstacle for development of atomic mobility in solid solder alloys is the lack of accurate diffusivity information. Taking the ternary Cu–Ag–Sn system for example, there is no any experimental diffusivity information for fcc phase available in the literature. Therefore, there is a need to remedy this situation.

The single-phase diffusion couple technique is frequently employed to determine the interdiffusivities of the target phase. For a ternary system, the well-known Matano–Kirkaldy method is the most widely used one in materials community [13–15]. With the Matano–Kirkaldy method, the four independent interdiffusivities at the intersection point along the diffusion paths of two diffusion couples can be obtained for a ternary system. Though the Matano–Kirkaldy method can give reasonable interdiffusivities, its efficiency is very low. With such a low efficiency, a large number of diffusion couple experiments should be performed if the composition-dependent interdiffusivities needs to be evaluated for a high-quality atomic mobility database. Moreover, its low efficiency cannot meet the requirement of abundant experimental data in the MGI (Materials Genome Initiative) [16,17] and/or ICME (Integrated Computational Materials Engineering) [18] projects nowadays. In order to solve this problem, a pragmatic numerical inverse method was developed and realized in a home-made code by Chen et al. [19] from our research group very recently. With such

* Corresponding author. Tel.: +86 731 88877963; fax: +86 731 88710855.

E-mail addresses: xueyun168@gmail.com, lijun.zhang@csu.edu.cn (L. Zhang).

a numerical inverse method, the composition-dependent interdiffusivities in ternary systems can be effectively determined by using a single diffusion couple. Thus, the efficiency increases dramatically in comparison with the traditional Matano–Kirkaldy method.

Consequently, high-throughput determination of the composition-dependent interdiffusivities in fcc Cu–Ag–Sn alloys is chosen as the target in the present work. The large amount of interdiffusivity information obtained in the present work will serve as the important basis for the establishment of atomic mobility database of fcc Cu–Ag–Sn system. The major objectives of the present work are (i) to determine the composition-dependent interdiffusivities in Cu-rich fcc Cu–Ag–Sn alloys at 1073 K by using the pragmatic numerical inverse method together with 5 groups of fcc single-phase Cu–Ag–Sn diffusion couples, and (ii) to validate the obtained composition-dependent interdiffusivities by comprehensively comparing with the results due to the Matano–Kirkaldy method as well as by Fick's second law applied to numerical simulation of composition profiles for each diffusion couple.

2. Experimental procedure

The terminal compositions of the five Cu–Ag–Sn diffusion couples are listed in Table 1. In order to make up the diffusion couples, binary/ternary alloys with terminal compositions need to be prepared first. Pure copper (purity: 99.99%), silver (purity: 99.99%), and tin (purity: 99.99%) were used as starting materials. Different amounts of pure metal elements Cu, Ag, and Sn corresponding to the terminal compositions were encapsulated in the separate vacuum quartz tubes. All the quartz tubes were then placed in a high-temperature furnace (GSL1700X, Hefei kejing materials technology Co., Ltd., Hefei, China) at 1473 K for 4 days to ensure that all the elements were molten. After cooling to room temperature, all the samples were then re-melted by arc melting under a high-purity argon atmosphere using a non-consumable tungsten electrode (WKDHL-1, Opto-electronics Co., Ltd., Beijing, China) for four times to improve their homogeneities. Subsequently, the samples were linearly cut into blocks of approximate dimensions $5 \times 5 \times 10 \text{ mm}^3$ after mechanically removing the surface material, and then sealed into an evacuated quartz tubes, and homogenized at $1073 \pm 5 \text{ K}$ for 20 days in an L4514-type diffusion furnace (Qingdao Instrument & Equipment Co., Ltd., China), followed by quenching in water. The polished and cleaned blocks were bound together by molybdenum wires to form five diffusion couples according to the assembly listed in Table 1. These couples were then sealed into quartz tubes under vacuum atmosphere, and annealed at 1073 K for 36 h in the L4514-type diffusion furnace. After that, the couples were quenched into cold water. The annealed couples were then metallographic polished along the planes parallel to diffusion direction. The solute concentration profiles of all the five diffusion couples were measured by means of EPMA technique (JXA-8230, JEOL, Japan) on the polished section.

3. Methods for evaluating ternary interdiffusion coefficients

In a hypothetical 1–2–3 ternary system (assuming 1 and 2 are solutes while 3 is chosen as the solvent. Here, the solvent is Cu, and the solutes are Ag and Sn), Fick's first and second law read as respectively

$$\tilde{J}_i = -\tilde{D}_{i1}^3 \frac{\partial c_1}{\partial x} - \tilde{D}_{i2}^3 \frac{\partial c_2}{\partial x} \quad (1)$$

$$\frac{\partial c_i}{\partial t} = \frac{\partial}{\partial x} \left(\tilde{D}_{i1}^3 \frac{\partial c_1}{\partial x} + \tilde{D}_{i2}^3 \frac{\partial c_2}{\partial x} \right) \quad (2)$$

Here, \tilde{J}_i is the interdiffusion flux of component i , c_1 and c_2 are the concentrations of solutes 1 and 2, x is the diffusion distance, and t is the time. \tilde{D}_{11}^3 and \tilde{D}_{22}^3 are the two main interdiffusion coefficients, while \tilde{D}_{12}^3 and \tilde{D}_{21}^3 are the two cross interdiffusion coefficients in the ternary system. In general, the interdiffusion coefficients are composition-dependent at a constant temperature (and pressure). As stated in Section 1, there are two methods to determine the composition-dependent interdiffusion coefficients in ternary systems, i.e., the pragmatic numerical inverse method and the Matano–Kirkaldy method, as briefly described in the following.

3.1. Pragmatic numerical inverse method

The pragmatic numerical inverse method was recently proposed by Chen et al. [19] to determine the composition-dependent interdiffusivities in ternary systems by using a single diffusion couple. According to Manning's random alloy model [20], the interdiffusivities \tilde{D}_{ij}^3 ($i, j = 1$ or 2) and the mobility M_i are related by:

$$\tilde{D}_{ij}^3 = RT \left[M_i \phi_{ij}^3 - c_i \left(M_1 \phi_{1j}^3 + M_2 \phi_{2j}^3 + M_3 \phi_{3j}^3 \right) \right] + s \left[\left(M_i - c_1 M_1 - c_2 M_2 - c_3 M_3 \right) \frac{2c_i RT \sum_m (M_m \phi_{mj}^3)}{A_0 \sum_m (c_m M_m)} \right] \quad (3)$$

where R is the gas constant and T is the temperature. ϕ_{ij}^3 is the thermodynamic factor, and can be expressed as:

$$\phi_{ij}^3 = \frac{c_i}{RT} \cdot \left(\frac{\partial \mu_i}{\partial c_j} - \frac{\partial \mu_i}{\partial c_3} \right) \quad (4)$$

where μ_i is the chemical potential of component i , and can be obtained from the corresponding thermodynamic descriptions, which are usually available for most alloy systems nowadays. The second part of Eq. (3) denotes the vacancy-wind effect, which considers the contribution of the vacancy flux. When s equals to 1, the vacancy-wind effect is considered. While s equals to 0, the vacancy-wind effect is not considered. The parameter A_0 is a factor depending only on crystal structure, and here equals to 7.15 for the face centered cubic (fcc) crystals [20]. The function developed by Andersson and Ågren [11] and incorporated in DICTRA software [21] was directly employed in the present work to express the atomic mobility for element i :

$$M_i = \frac{1}{RT} \exp \left(\frac{\Delta G_i}{RT} \right) \quad (5)$$

where ΔG_i can be expanded by the Redlich–Kister polynomial:

$$\Delta G_i = c_1 \Delta G_i^1 + c_2 \Delta G_i^2 + c_3 \Delta G_i^3 + c_1 c_2 \Delta G_i^{1,2} + c_1 c_3 \Delta G_i^{1,3} + c_2 c_3 \Delta G_i^{2,3} + c_1 c_2 c_3 \Delta G_i^{1,2,3} \quad (6)$$

Here, ΔG_i^1 , ΔG_i^2 and ΔG_i^3 are the end-members for diffusion of element i in elements 1, 2 and 3, while $\Delta G_i^{1,2}$, $\Delta G_i^{1,3}$, $\Delta G_i^{2,3}$ and $\Delta G_i^{1,2,3}$ are the interaction parameters for the mobility of element i in the 1–2, 1–3, 2–3 and 1–2–3 systems, respectively. For

Table 1
List of terminal compositions of the five diffusion couples in the present work.

Couple name	Composition (at.%)	Temperature (K)	Diffusion time (hours)
C1	Cu–1.8Sn/Cu–1.9Ag	1073	36
C2	Cu/Cu–1.7Sn–2.6Ag	1073	36
C3	Cu/Cu–3.8Sn–1.0Ag	1073	36
C4	Cu–2.9Sn/Cu–2.0Ag	1073	36
C5	Cu–1.98Sn/Cu–3.5Ag	1073	36

simplicity, the end-members corresponding to self and impurity diffusivities are fixed by using the experimental data, first-principles calculations, molecular dynamic simulation or some semi-empirical relations. The other coefficients such as $\Delta G_i^{1,2}$, $\Delta G_i^{1,3}$, $\Delta G_i^{2,3}$ and $\Delta G_i^{1,2,3}$ are treated as adjustable parameters. Moreover, only one or two of them are needed to be evaluated in most cases for one diffusion couple. Therefore, by combining Eqs. (2)–(6), one can evaluate the composition-dependent interdiffusivities based on the measured concentration profiles together with the available thermodynamic description.

During the evaluation of interdiffusivities, the Fick’s second law was applied to simulate the concentration profiles based on the computed interdiffusivities, an optimal set of adjustable parameters such as $\Delta G_i^{1,2}$, $\Delta G_i^{1,3}$, $\Delta G_i^{2,3}$ and/or $\Delta G_i^{1,2,3}$ were carefully chosen by iteratively fitting until the minimization of the error between the measured and the simulated concentration profiles is achieved:

$$\min \langle \text{error} \rangle = \min \left\langle \frac{1}{N} \sum_{i=1,2} \sum_{j=1}^N \left(|c_{ij}^{\text{cal}} - c_{ij}^{\text{exp}}| \right) \right\rangle \quad (7)$$

where c_{ij}^{cal} and c_{ij}^{exp} are the calculated and the experimental concentrations of component i at the j th point, respectively, and N is the total number of the experimental data. With the optimal set of the fitting parameters, the concentration-dependent interdiffusivities in the target ternary system can be computed via Eq. (3).

3.2. Matano–Kirkaldy method

Based on the Fick’s first law in Eq. (1), Kirkaldy successfully extended the Boltzmann–Matano method into ternary and even higher-order systems [13,14].

Assuming that each component has the same molar volume, the interdiffusion flux of each component can be determined directly from the concentration profiles without using the interdiffusion coefficients [22]. The interdiffusion flux of component i can be expressed as:

$$\tilde{J}_i = \frac{1}{2t} \int_{c_i^{-\infty}}^{c_i^{+\infty}} (x - x_0) dc_i \quad (8)$$

where t is the diffusion time, x_0 is the position of Matano plane [13,14] and can be obtained from the following relation:

$$\int_{c_i^{-\infty}}^{c_i^{+\infty}} (x - x_0) dc = 0 \quad (9)$$

and $c_i^{-\infty}$ and $c_i^{+\infty}$ ($i = 1, 2$) are the terminal compositions at the left and right sides of the diffusion couple. The initial and boundary conditions for the semi-infinite diffusion couples are:

$$c_i(\pm x, 0) = c_i(\pm \infty, t) = c_i^{\pm \infty} \quad (10)$$

Combining Eqs. (1) and (8), one can obtain:

$$\int_{c_i^{-\infty}}^{c_i^{+\infty}} (x - x_0) dc_i = -2t \left(\tilde{D}_{i1}^3 \frac{dc_1}{dx} + \tilde{D}_{i2}^3 \frac{dc_2}{dx} \right)_{c_i} \quad (11)$$

With four equations similar to Eq. (11) from two diffusion couples, the four main and cross interdiffusivities in Eq. (1) of the intersection point can be then determined.

4. Results and discussion

Considering that all the 5 diffusion couples are in the same fcc single-phase region, one typical microstructure of the diffusion zone is given in Fig. 1, which shows the backscattered electron image (BEI) of C5 (Cu–1.98Sn/Cu–3.5Ag) diffusion couple annealed at 1073 K for 36 h. The concentration profiles of each component in

all the 5 diffusion couples measured by EPMA in the present work are presented in Fig. 2. Based on Eqs. (8) and (9), the corresponding interdiffusion fluxes in these diffusion couples can be also calculated and presented in Fig. 2. It should be noted that all the experimental data are denoted in symbols.

Based on the measured composition profiles, the composition-dependent interdiffusivities of fcc Cu–Ag–Sn alloys at 1073 K along the entire diffusion path of each diffusion couple were then effectively determined by using the pragmatic numerical inverse method. During the evaluation of the interdiffusivities, the thermodynamic descriptions for fcc phase in the Ag–Cu–Sn system were directly taken from Kattner [23], from which the thermodynamic factor in Eq. (4) can be provided. While the end-members for the three binary systems, ΔG_i^1 , ΔG_i^2 and ΔG_i^3 , were taken from Refs. [24–26], and fixed all the time. Moreover, the vacancy-wind effect was considered in the present work. One or two of the adjustable parameters, $\Delta G_i^{1,2}$, $\Delta G_i^{1,3}$, $\Delta G_i^{2,3}$ and $\Delta G_i^{1,2,3}$, were tried to get the best fit to the experimental composition profiles for each diffusion couple. With the final optimal set of adjustable parameters for each diffusion couple, the ternary interdiffusivities of composition dependence can be directly calculated by using Eqs. (2)–(6). All the calculated interdiffusivities were subject to the examination of the following thermodynamically stable constraints [27],

$$\tilde{D}_{\text{SnSn}}^{\text{Cu}} + \tilde{D}_{\text{AgAg}}^{\text{Cu}} > 0 \quad (12)$$

$$\tilde{D}_{\text{SnSn}}^{\text{Cu}} \cdot \tilde{D}_{\text{AgAg}}^{\text{Cu}} - \tilde{D}_{\text{SnAg}}^{\text{Cu}} \cdot \tilde{D}_{\text{AgSn}}^{\text{Cu}} \geq 0 \quad (13)$$

$$\left(\tilde{D}_{\text{SnSn}}^{\text{Cu}} - \tilde{D}_{\text{AgAg}}^{\text{Cu}} \right)^2 + 4 \cdot \tilde{D}_{\text{SnAg}}^{\text{Cu}} \cdot \tilde{D}_{\text{AgSn}}^{\text{Cu}} \geq 0 \quad (14)$$

Only those interdiffusivities fulfill the above constraints can be output.

The finally obtained ternary interdiffusivities, $\tilde{D}_{\text{SnSn}}^{\text{Cu}}$, $\tilde{D}_{\text{SnAg}}^{\text{Cu}}$, $\tilde{D}_{\text{AgSn}}^{\text{Cu}}$ and $\tilde{D}_{\text{AgAg}}^{\text{Cu}}$ for the 5 fcc Cu–Ag–Sn diffusion couples are presented in Fig. 3 as a three-dimensional (3-D) illustration. For readers’ convenient usage, all the original experimental data are also provided as the electronic [Supplementary Materials](#). The errors of the interdiffusivities determined by the pragmatic numerical inverse method were evaluated according to the scientific method proposed by Lechelle et al. [28], who considered the error propagation via the following function,

$$u(f(A, B \dots)) = \sqrt{\sum_{\alpha=A, B \dots} \left(\frac{\partial f}{\partial \alpha} \right)^2 (u(\alpha))^2} \quad (15)$$

Here, A and $B \dots$ are the correlation quantities of function f like Eqs. (3) and (5), while $u(\alpha)$ ($\alpha = A, B \dots$) is the uncertainty of variable α like concentration. During the evaluation of the errors, the differences between the experimental concentration profiles and the predicted ones propagate to calculation of atomic mobility in Eq. (5) and then to calculation of diffusivities in Eq. (3). In order to eliminate the effect of the absolute value, the relative error (i.e., equals to the uncertainty divided by the absolute value of the interdiffusivity) rather than the uncertainty itself was utilized in the present work. Moreover, considering that one relative error can be determined for one diffusivity, numerous errors should be evaluated, displayed and stored. For a clear display of the concentration-dependent diffusivities along the entire diffusion paths, as well as to save the space, only the average error of the diffusivities was provided here for simplification. The average relative error of the interdiffusivities obtained by this numerical inverse method was finally evaluated to be 8%. It can be clearly seen from Fig. 3 that the ternary interdiffusivities for all the diffusion couples vary apparently along with the composition of Sn and Ag. All the

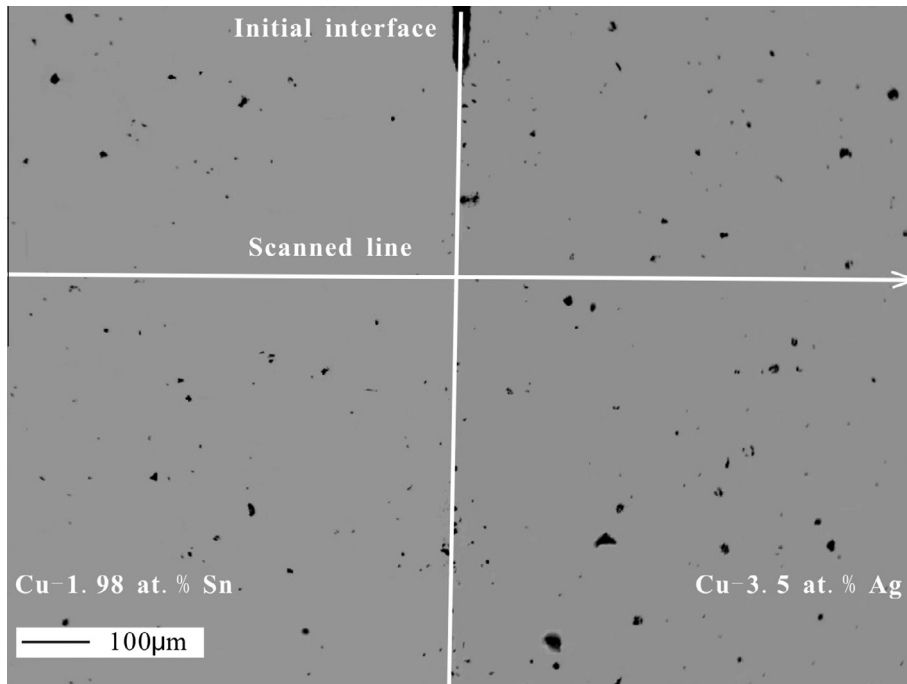


Fig. 1. Backscattered electron image of the microstructure of the Cu-1.98Sn/Cu-3.5Ag diffusion couple annealed at 1073 K for 36 h.

main interdiffusivities determined by the pragmatic numerical inverse method are positive, while all the cross ones are negative. According to the thermodynamic analysis by Liu et al. [29], the negative sign of the cross interdiffusivities indicates a negative gradient of diffusion potentials versus composition. Moreover, the main interdiffusivity $\tilde{D}_{\text{SnSn}}^{\text{Cu}}$ is larger than the other main one $\tilde{D}_{\text{AgAg}}^{\text{Cu}}$, which indicates that the diffusion rate of Sn in the fcc Cu–Ag–Sn alloys at 1073 K is faster than that of Ag. In addition, one more nice feature of such 3-D plot in Fig. 3 is that the projection of the interdiffusivities for each diffusion couple on the composition plane is exactly the diffusion path of the respective diffusion couple. In order to further provide a quantitative description of how the diffusivities vary with concentrations and also give an idea of the scatter in the diffusivity data, the contour maps for the obtained interdiffusivities are plotted and displayed in Fig. 4. As can be seen in the figure, the variation of the main interdiffusivities $\tilde{D}_{\text{SnSn}}^{\text{Cu}}$ and $\tilde{D}_{\text{AgAg}}^{\text{Cu}}$, and the absolute values of cross interdiffusivity $\tilde{D}_{\text{SnAg}}^{\text{Cu}}$ depends heavily on Sn content, while that of the absolute values of cross interdiffusivity $\tilde{D}_{\text{AgSn}}^{\text{Cu}}$ depends heavily on Ag content. Moreover, the main interdiffusivities $\tilde{D}_{\text{SnSn}}^{\text{Cu}}$ and $\tilde{D}_{\text{AgAg}}^{\text{Cu}}$, and the absolute values of cross interdiffusivity $\tilde{D}_{\text{SnAg}}^{\text{Cu}}$ increase as Sn content increases. However, the absolute values of cross interdiffusivity $\tilde{D}_{\text{AgSn}}^{\text{Cu}}$ decrease as Ag content increases.

Based on the obtained composition-dependent interdiffusivities along the entire diffusion path, the composition profiles for each diffusion couple can be simulated by using Fick's second law (i.e., Eq. (2)). The simulated composition profiles of Cu, Ag and Sn for each diffusion couple annealed at 1073 K for 36 h are compared with the corresponding experimental data, as shown in Fig. 2. As can be seen from the figure, the simulated concentration profiles are in excellent agreement with the experimental data. Moreover, on the basis of the simulated composition profiles for each diffusion couple together with either Eqs. (1) or (8), the corresponding interdiffusion fluxes of each elements can be directly computed, as also presented in Fig. 2. Again, the agreement

between the calculated interdiffusion fluxes and the experimental data is fairly good. Both facts in Fig. 2 indicate that the presently obtained interdiffusivities by using the numerical inverse method are reasonable.

In order to further validate the reliability of the obtained interdiffusivities, the Matano–Kirkaldy method was utilized to calculate the interdiffusivities at the specific intersection points of the diffusion paths for all the 5 diffusion couples. Based on Fig. 3, there are totally 7 intersection points of the diffusion paths. But the intersection points of C1/C3 and C3/C5 diffusion couples, as well as those of C2/C4, C2/C5 and C4/C5 diffusion couples, are close to each other, these intersection points are approximately supposed to be one point. Thus, the interdiffusivities for the total 4 intersection points were then determined. Considering that all the measured concentration profiles of Sn and Ag are almost symmetric, the standard Boltzmann function,

$$c(x) = \frac{A_1 - A_2}{1 + e^{(x-x_0)/dx}} + A_2 \quad (16)$$

was used to fit the experimental profiles of Sn and Ag and generate the smooth concentration profiles $c_i(x)$ relative to the distance. Here, A_1 , A_2 and dx are the fitting parameters for each concentration profile. Moreover, the position of Matano plane x_0 here should be an average one of Sn and Ag in one diffusion couple. And the fitted concentration profiles of Cu were obtained based on the relationship $x_{\text{Cu}} = 1 - x_{\text{Ag}} - x_{\text{Sn}}$. Based on the fitted Boltzmann functions together with the above-mentioned Matano–Kirkaldy method, the four interdiffusivities at the interaction point of the diffusion path for the two diffusion couples can be then obtained. All the finally obtained interdiffusivities by the Matano–Kirkaldy method are listed in Table 2. Moreover, the uncertainty of the interdiffusivities was also evaluated according to the scientific method by Lechelle et al. [28]. During the evaluation of uncertainties of the interdiffusivities by the Matano–Kirkaldy method, the uncertainties of the elemental concentrations due to different sources, like the experimental measurement and the Boltzmann function fitting, firstly propagated to calculation of the interdiffusion fluxes (e.g., Eq. (8))

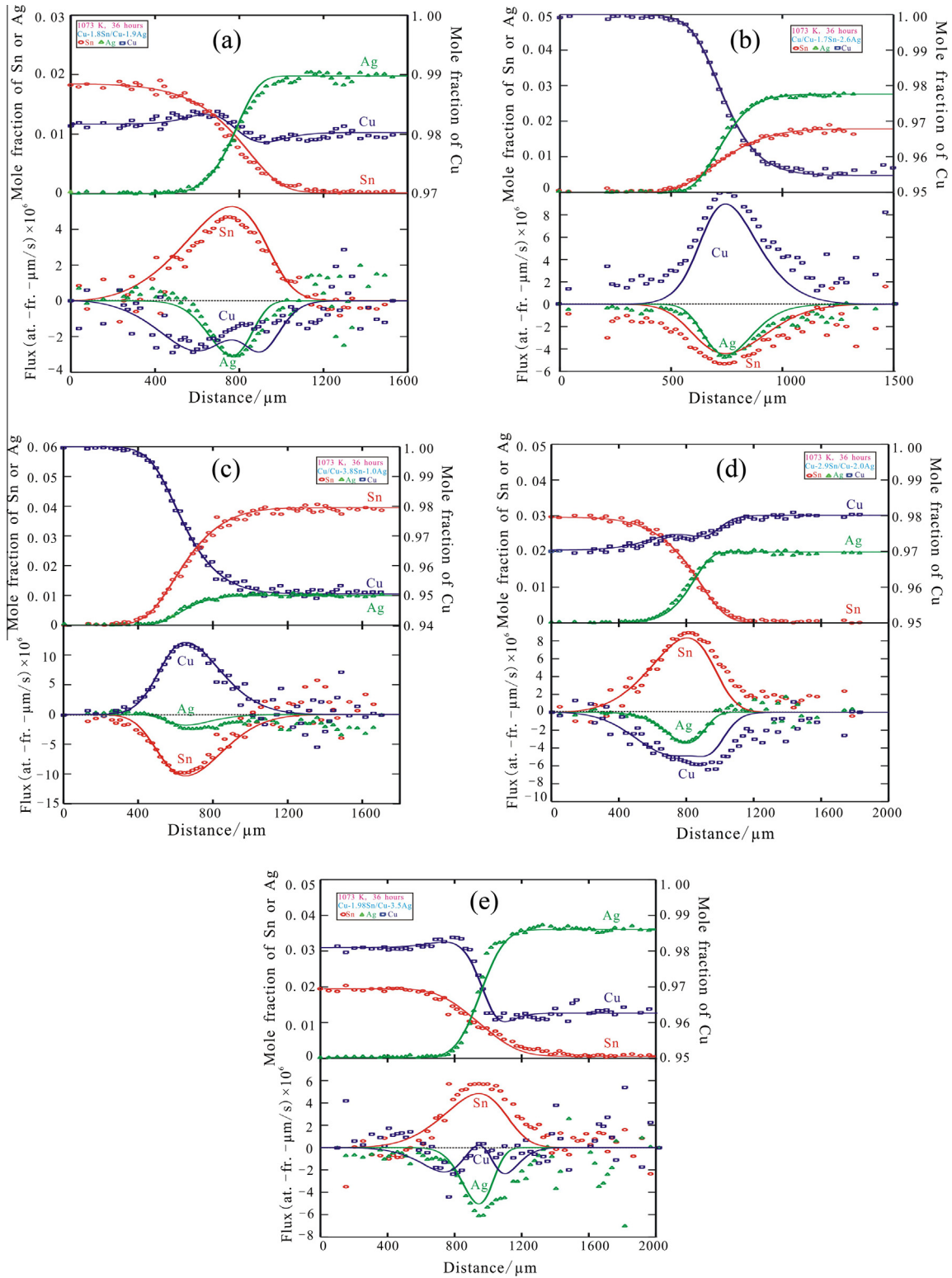


Fig. 2. Comparison between the experimental and the simulated concentration profiles/interdiffusion fluxes of the diffusion couples annealed at 1073 K for 36 h based on the ternary interdiffusion coefficients obtained in the present work; (a) C1: Cu–1.8Sn/Cu–1.9Ag, (b) C2: Cu/Cu–1.7Sn–2.6Ag, (c) C3: Cu/Cu–3.8Sn–1.0Ag, (d) C4: Cu–2.9Sn/Cu–2.0Ag, and (e) C5: Cu–1.98Sn/Cu–3.5Ag. Symbols are due to the experimental measurement.

and then to calculation of the interdiffusivities (e.g., Eq. (11)). Again, the relative error (i.e., equals to the uncertainty divided by the absolute value of the interdiffusivity) rather than the uncertainty itself was utilized here. The finally relative errors for the interdiffusivities evaluated by the Matano–Kirkaldy method are also listed in Table 2.

In order for a direct comparison, the interdiffusivities at the same compositions calculated by using pragmatic numerical inverse method were also listed in Table 2. It can be seen from the table that (i) there exists differences (lower than 50% in general) among the interdiffusivities measured at nearly the same composition by

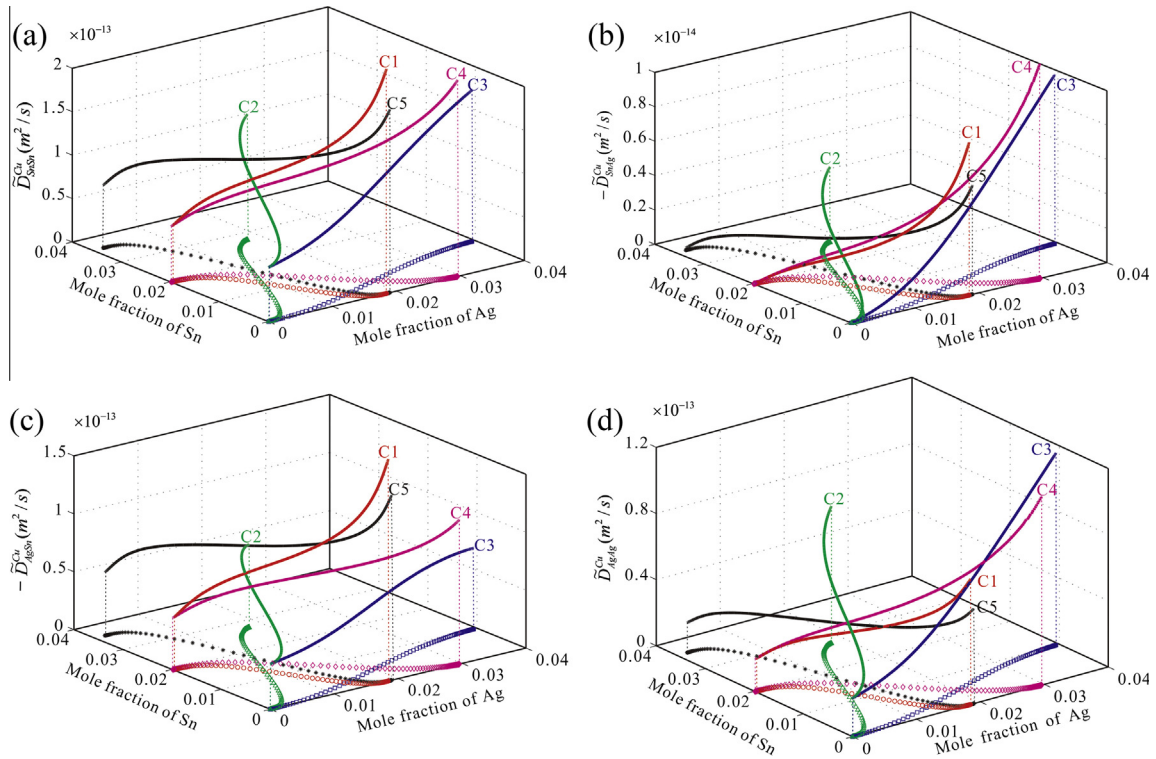


Fig. 3. 3-D illustration of the obtained ternary interdiffusivities along the entire diffusion paths based on the numerical inverse method in the present work: (a) \bar{D}_{SnSn}^{Cu} , (b) $-\bar{D}_{SnAg}^{Cu}$, (c) $-\bar{D}_{AgSn}^{Cu}$, and (d) \bar{D}_{AgAg}^{Cu} .

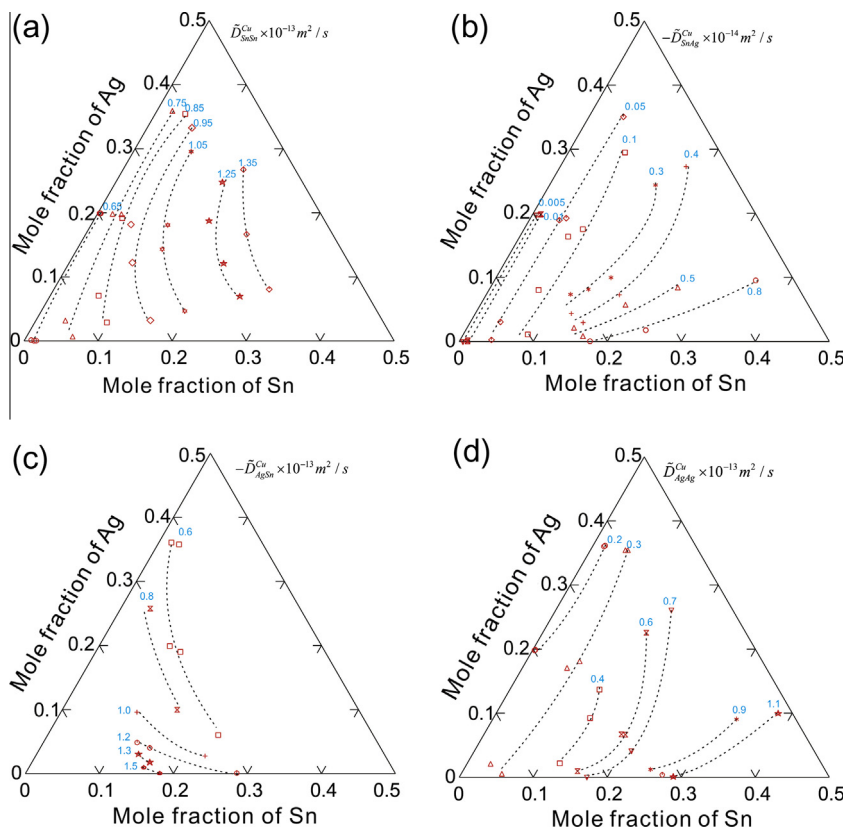


Fig. 4. Contour maps for the obtained ternary interdiffusivities based on the numerical inverse method in the present work: (a) \bar{D}_{SnSn}^{Cu} , (b) $-\bar{D}_{SnAg}^{Cu}$, (c) $-\bar{D}_{AgSn}^{Cu}$, and (d) \bar{D}_{AgAg}^{Cu} . The points denote the interdiffusivities evaluated by the numerical inverse method in the present work. The dashed iso-diffusivity lines are drawn by hand based on the points.

Table 2
Diffusion coefficients in Cu-rich fcc Cu–Ag–Sn alloys obtained in this work.

Compositions (at.%)		Diffusion coefficients ($10^{-14} \text{ m}^2 \text{ s}^{-1}$)								Couple name
Sn	Ag	Matano–Kirkaldy method				Numerical inverse method				
		$\bar{D}_{\text{SnSn}}^{\text{Cu}}$ (RE) ^a	$\bar{D}_{\text{SnAg}}^{\text{Cu}}$ (RE) ^a	$\bar{D}_{\text{AgSn}}^{\text{Cu}}$ (RE) ^a	$\bar{D}_{\text{AgAg}}^{\text{Cu}}$ (RE) ^a	$\bar{D}_{\text{SnSn}}^{\text{Cu}}$ (RE: 8%) ^b	$\bar{D}_{\text{SnAg}}^{\text{Cu}}$ (RE: 8%) ^b	$\bar{D}_{\text{AgSn}}^{\text{Cu}}$ (RE: 8%) ^b	$\bar{D}_{\text{AgAg}}^{\text{Cu}}$ (RE: 8%) ^b	
1.012	1.619	12.54	−1.25	−1.89	4.01	10.25	−0.18	−5.68	4.92	C2
		(2.93%)	(14.95%)	(7.28%)	(2.74%)	9.94	−0.15	−6.65	3.51	C4
						12.15	−0.17	−9.26	3.12	C5
1.337	0.323	10.97	−1.38	−0.29	5.55	17.75	−0.43	−12.86	5.36	C1
		(2.77%)	(26.80%)	(26.72%)	(6.27%)	9.31	−0.21	−5.19	4.34	C3
						15.7	−0.35	−11.68	4.37	C5
1.999	0.594	11.14	−1.65	−0.15	5.34	10.86	−0.33	−5.74	5.49	C3
		(2.72%)	(25.62%)	(4.57%)	(4.02%)	14.96	−0.50	−9.08	6.45	C4
0.810	1.103	11.17	−0.74	−2.37	3.94	11.92	−0.16	−8.66	3.49	C1
		(2.63%)	(17.3%)	(9.17%)	(2.56%)	9.22	−0.13	−5.18	4.28	C2

^a Here, 'RE' means the relative error of each interdiffusivity obtained by the Matano–Kirkaldy method.

^b Here, 'RE: 8%' means the average error of the interdiffusivities obtained by the numerical inverse method is 8%.

different sets of diffusion couples via the pragmatic numerical inverse method. That is because in such inverse method the concentration gradient has effect on the evaluated interdiffusivities [30,31]. For the same composition, the compositions gradients (and also interdiffusion flux gradients) in different diffusion couples are completely different (see Fig. 2). However, a further analysis of the data indicate that such effect can be eliminated if the model-predicted concentration profiles can reproduce the experimental data exactly. For instance, the model-predicted concentration profiles of couple 3 fit better to the experimental data than those of couples 1 and 5. The diffusivities obtained from couple 3 are closer to the diffusivities obtained by the Matano–Kirkaldy method than those from couples 1 and 5; (ii) the main interdiffusivities at the intersection points by these two methods are almost the same, while the cross interdiffusivities show some differences. Actually, such a difference is normal because it is well-known that the cross interdiffusivities cannot be precisely determined by the traditional Matano–Kirkaldy method. Therefore, it can be concluded that the presently obtained interdiffusivities by using the numerical inverse method are reliable.

5. Conclusions

Five bulk diffusion couples in Cu-rich fcc Cu–Ag–Sn alloys at 1073 K were prepared and measured by means of EPMA technique in the present work. The composition-dependent interdiffusivity matrices along the entire diffusion paths of the five fcc Cu–Ag–Sn diffusion couples were obtained by using the recently proposed pragmatic numerical inverse method. The reliability of the obtained ternary interdiffusivities was verified by thermodynamic stable constraints and sensitive interdiffusion fluxes, Fick's second law applied to numerical simulation as well as comparisons with the interdiffusivities obtained by the Matano–Kirkaldy method. The good agreement was observed, indicating that the interdiffusivities in Cu-rich fcc Cu–Ag–Sn alloys at 1073 K determined by the pragmatic numerical inverse method are reliable.

Acknowledgements

The financial support from the National Natural Science Foundation for Youth of China (Grant No. 51301208), the National Natural Science Foundation of China (Grant No. 51474239) and the National Basic Research Program of China (Grant No. 2014CB644002) is greatly acknowledged. This research is jointly sponsored by Guangxi Key Laboratory of Information Materials (Guilin University of Electronic Technology), People's Republic of China (Project No. 131004-K). Lijun Zhang

acknowledges the support from Shenghua Scholar Program of Central South University, China.

Appendix A. Supplementary material

Supplementary data associated with this article can be found, in the online version, at <http://dx.doi.org/10.1016/j.jallcom.2015.05.030>.

References

- [1] P.T. Vianco, D.R. Frear, *JOM* 45 (1993) 14–19.
- [2] H.-T. Ma, J. Wang, L. Qu, N. Zhao, A. Kunwar, *J. Electron. Mater.* 42 (2013) 2686–2695.
- [3] A. Milosavljević, D. Živković, D. Manasijević, Y. Du, N. Talijan, M. Bu, A. Kostov, *Int. J. Mater. Res.* 104 (2013) 452–456.
- [4] A.A. El-Daly, A.M. El-Taher, S. Gouda, *J. Alloys Comp.* 627 (2015) 268–275.
- [5] L. Ye, Z.H. Lai, J. Liu, A. Thölen, *Solder. Surf. Mt. Technol.* 13 (2001) 16–20.
- [6] A.A. El-Daly, A.E. Hammad, G.S. Al-Ganainy, M. Ragab, *J. Alloys Comp.* 614 (2014) 20–28.
- [7] W.M. Chen, L. Zhang, D.D. Liu, Y. Du, C.Y. Tang, *J. Electron. Mater.* 42 (2013) 1158–1170.
- [8] W.M. Chen, L. Zhang, Y. Du, B.Y. Huang, *J. Electron. Mater.* 43 (2014) 1131–1143.
- [9] W.M. Chen, L. Zhang, Y. Du, B.Y. Huang, *Int. J. Mater. Res.* 105 (2014) 827–839.
- [10] W.M. Chen, L. Zhang, Y. Du, B.Y. Huang, *Philos. Mag.* 94 (2014) 1552–1577.
- [11] J.O. Andersson, J. Ågren, *J. Appl. Phys.* 72 (1992) 1350–1355.
- [12] L. Zhang, Y. Du, I. Steinbach, Q. Chen, B.Y. Huang, *Acta Mater.* 58 (2010) 3664–3675.
- [13] J.S. Kirkaldy, J.E. Lane, G.R. Masson, *Can. J. Phys.* 41 (1963) 2174–2186.
- [14] J.S. Kirkaldy, D.J. Young, *Diffusion in the Condensed State*, Institute of Metals, London, 1987.
- [15] L. Zhang, D. Liu, W. Zhang, S. Wang, Y. Tang, N. Ta, M. Wei, Y. Du, *Mater. Sci. Forum* 794–796 (2014) 611–616.
- [16] L. Kaufman, J. Ågren, *Scripta Mater.* 70 (2014) 3–6.
- [17] G.B. Olson, C.J. Kuehmann, *Scripta Mater.* 70 (2014) 25–30.
- [18] G. Gottstein, *Integral Materials Modeling: Towards Physics-Based Through-Process Models*, Wiley-VCH Verlag GmbH&Co. KGaA, Germany, 2007.
- [19] W.M. Chen, L. Zhang, Y. Du, C.Y. Tang, B.Y. Huang, *Scripta Mater.* 90–91 (2014) 53–56.
- [20] J.R. Manning, *Metall. Trans.* 1 (1970) 499–505.
- [21] A. Borgenstam, A. Engström, L. Höglund, J. Ågren, *J. Phase Equilib.* 21 (2000) 269–280.
- [22] M.A. Dayananda, *Metall. Trans. A* 14 (1983) 1851–1858.
- [23] U. Kattner, *Solder Database (solder.tdb)*, NIST, <<http://www.metallurgy.nist.gov/phase/solder/solder.html>>.
- [24] Y.J. Liu, J. Wang, Y. Du, G. Sheng, L.J. Zhang, D. Liang, *Calphad* 35 (2011) 224–230.
- [25] J. Wang, C. Leinenbach, H.S. Liu, L.B. Liu, M. Roth, Z.P. Jin, *Calphad* 33 (2009) 704–710.
- [26] Y.J. Liu, J. Wang, Y. Du, G. Sheng, L.J. Zhang, D. Liang, *Calphad* 35 (2011) 314–322.
- [27] L. Onsager, *Ann. N. Y. Acad. Sci.* 46 (1945) 241–265.
- [28] J. Lechelle, S. Noyau, L. Aufore, A. Arredondo, E. Audubert, *Diffus. Fundam. Org.* 17 (2012) 1–39.
- [29] D.D. Liu, L.J. Zhang, Y. Du, H.H. Xu, Z.P. Jin, *J. Alloys Comp.* 566 (2013) 156–163.
- [30] J.E. Morral, W.D. Hopfe, *J. Phase Equilib. Diffus.* 35 (2014) 666–669.
- [31] A.V. Jaques, J.C. LaCombe, *J. Phase Equilib. Diffus.* 33 (2012) 181–188.